Eur. Phys. J. B **42**, 441–450 (2004)
DOI: 10.1140/epjb/e2004-00402-8

THE EUROPEAN PHYSICAL JOURNAL B

(2+1) dimensional Hărăgus-Courcelle-Il'ichev model for the liquid surface waves in the presence of sea ice or surface tension: Bäcklund transformation, exact solutions and possibly observable effects

Bo Tian[1,2] and Yi-Tian Gao[3,4,2,a]

[1] School of Science, P.O. Box 122, Beijing University of Posts and Telecommunications, Beijing 100876, China
[2] State Key Laboratory of Software Development Environment, Beijing University of Aeronautics and Astronautics, Beijing 100083, China
[3] CCAST (World Lab.), P.O. Box 8730, Beijing 100080, China
[4] Ministry of Education Key Laboratory of Fluid Mechanics and National Laboratory for Computational Fluid Dynamics, Beijing University of Aeronautics and Astronautics, Beijing 100083, China[b]

Received 21 July 2004
Published online 23 December 2004 –

Abstract. The wave propagation on an ocean or water surface in the presence of sea ice or surface tension is of current importance. In this paper, we investigate the (2+1) dimensional 6th-order model proposed recently by Hărăgus-Courcelle and Il'ichev for such wave propagation. Firstly, we correct some errors in the original derivations of this model. With computerized symbolic computation and truncated Painlevé expansion, we then obtain an auto-Bäcklund transformation and types of the solitonic and other exact analytic solutions to the model, with the solitary waves as a special case, able to be dealt with the powerful Wu method. Based on the results, we later propose some possibly observable effects for the future experiments, and in the end, provide a possible way to explain the regular structure of the open-sea ice break-up observations.

PACS. 47.11.+j Computational methods in fluid dynamics – 05.45.Yvi Solitons – 47.35.+i Hydrodynamic waves – 02.70.Wz Symbolic computation (computer algebra)

1 Introduction

Recently, people devote their attention to the wave propagation on an ocean or water surface in the presence of sea ice or surface tension. From the engineering standpoint, the water-ice (or, flexural-gravity) waves are of practical value in the studies on, e.g., the ice growth on structures, damage to offshore constructions by floating ice sheets, stress control for the facilities built upon the ice, and performance of ice-breaking ships [1–8]. In the gravity-capillary case, comparison of theoretical results and experimental data is relatively hard to perform, as seen, e.g., in reference [9].

Theoretical models of gravity-capillary and flexural-gravity waves have been provided by, e.g., references [6,10–12], among which the (2+1) dimensional Hărăgus-Courcelle-Il'ichev model [5,6],

$$u_{xt}+(uu_x)_x+su_{xxxx}+u_{xxxxxx}+u_{yy}=0,\ \ s=\pm1, \quad (1)$$

has been recently proposed, where x, y and t are dimensionless spatial and temporal variables, and u is a dimensionless surface deviation. Equation (1) is derived from the (2+1) dimensional system of Euler equations for long gravity-capillary waves of small amplitude when the dimensionless Bond number b is close to $\frac{1}{3}$ (in the presence of surface tension), and also for surface water waves in the presence of a floating elastic ice plate. In fact, the experiments [1] indicate that an ice sheet exhibits an elastic behavior for a wide set of physical conditions. For Bond numbers $b > \frac{1}{3}$, as well as for elastic plates with large initial tensions, $s = -1$; In the other case, for water waves with $b < \frac{1}{3}$ and elastic plates with low initial tensions, $s = 1$. The derivations of equation (1) have been given in reference [5] from those different cases, characterized by different s in the end.

Equation (1) generalizes the Kadomtsev-Petviashvili equation to the presence of higher order dispersive effects, as well as generalizes the fifth order Korteweg-de Vries equation into (2+1) dimensions. These effects are caused either by a surface tension with Bond number close to 1/3, or by an elastic ice-sheet floating on the water surface [5–7]. Topics on the Kadomtsev-Petviashvili equation can be found, e.g., in references [13–18], while on the fifth order Korteweg-de Vries equation, e.g., in references [5,11,19,20].

[a] e-mail: gaoyt@public.bta.net.cn
[b] Mailing address for YTG

For equation (1), reference [5] presents several approximate analytic solitary-wave solutions subject to either periodic or Dirichlet boundary conditions in the direction transverse to the propagation (i.e., the y direction), which have damped oscillations and propagate in a channel (along the x-axis). The instability treatment in [6] indicates that the periodic waves subject to the x-homogeneous, y-axis perturbations, also analytic but approximate, are found to decay into a sequence of parallel wave guides or channels, each of which represents the wave propagating along the x axis but localized in the y direction. It has been claimed [6] that such a self-channeling effect could help explain the regular structure of ice break-up. For $s = -1$, reference [21] proposes some possibly observable effects for the soliton-like liquid wave propagation in the presence of surface tension. Other related work includes the instability and collapse of waveguides on the water surface under the ice cover [8].

Symbolic computation is a new branch of artificial intelligence, with its remarkable feature as the permeation of computer sciences among various fields of science and engineering. Symbolic computation drastically increases the ability of a computer to exactly and algorithmically deal with the expressions, so that it is thought as the sign of modern scientific computations [22].

In Section 2 of this paper, we will correct some errors in the derivations of equation (1); From Section 3 to Section 5, we will work out certain exact analytic solutions and an auto-Bäcklund transformation to equation (1); Section 6 will be our discussion part, where we try to provide a way to explain the regular structure of the sea ice break-up observations, and to propose more possibly observable effects for the future experiments.

2 Investigation on the derivations leading to equation (1)

We hereby point out that there appear some errors in reference [5] on the derivations leading to equation (1). Our corrections are as follows:

Starting from the beginning, the third equation of the full system of Euler equations, i.e., equations (2.1) presented in reference [5], should be

$$\eta_t + \eta_x\,\phi_x + \eta_y\,\phi_y = \phi_z. \tag{2}$$

The Euler system is then transformed into equation (2.2) in reference [5], the fourth equation of which should be

$$\phi_t + \frac{1}{2}\,\epsilon\left(\phi_x^2 + \phi_y^2 + \phi_z^2/\mu\right) + \eta - \beta\,\triangle_{xy}\eta + \gamma\,\triangle_{xy}^2\eta + \delta\,\eta_{tt} = 0. \tag{3}$$

Equation (2.5) in reference [5] come out after the expansions in power series for small μ and z. The correct form of equations (2.5) should be

$$\eta_t + \epsilon\,\eta_x\,\phi_x + \epsilon\,\eta_y\,\phi_y + \triangle_{xy}\phi + \frac{\mu}{3}\,\triangle_{xy}^2\phi + \frac{2}{15}\,\mu^2\,\triangle_{xy}^2\phi + \frac{2}{15}\,\mu^2\,\triangle_{xy}^2\phi = 0, \tag{4}$$

$$\phi_t + \frac{\epsilon}{2}\,\left(\phi_x^2 + \phi_y^2\right) + \eta - \beta\,\triangle_{xy}\eta + \gamma\,\triangle_{xy}^2\eta + \delta\,\eta_{tt} = 0. \tag{5}$$

Having considered

$$\eta = \eta_0 + \mu\,\eta_1 + \mu^2\,\eta_2 + O(\mu^3), \tag{6}$$

$$\phi = \phi_0 + \mu\,\phi_1 + \mu^2\,\phi_2 + O(\mu^3). \tag{7}$$

Reference [5] looks for the waves travelling in one direction in the reference frame

$$\eta = \hat{\eta}\,(\xi,\zeta,\tau,\mu)\,, \qquad \phi = \hat{\phi}\,(\xi,\zeta,\tau,\mu)\,,$$
$$\xi = x - t, \qquad \zeta = \sqrt{\epsilon}\,y, \qquad \tau = \mu^m\,t, \qquad m > 0, \tag{8}$$

and investigates separately the following two cases:

(1) Long water waves beneath an ice sheet. Let $m = 1$, $\delta = \hat{\delta}\,\mu$, $\gamma = \hat{\gamma}\,\mu$, $\epsilon = \hat{\epsilon}\,\mu$, $\beta = 0$, and reference [5] obtains two equations between equations (2.6) and (2.7), which should be corrected as

$$-\hat{\eta}_{0\xi} - \mu\,\hat{\eta}_{1\xi} + \mu\,\hat{\eta}_{0\tau} + \hat{\epsilon}\,\mu\,\hat{\eta}_{0\xi}\,\hat{\phi}_{0\xi} + \hat{\phi}_{0\xi\xi} + \mu\,\hat{\phi}_{1\xi\xi} + \hat{\epsilon}\,\mu\,\hat{\phi}_{0\zeta\zeta} + \frac{\mu}{3}\,\hat{\phi}_{0\xi\xi\xi\xi} = 0,$$

$$-\hat{\phi}_{0\xi} - \mu\,\hat{\phi}_{1\xi} + \mu\,\hat{\phi}_{0\tau} + \frac{\hat{\epsilon}\,\mu}{2}\,\hat{\phi}_{0\xi}^2 + \hat{\eta}_0 + \mu\,\hat{\eta}_1 + \hat{\delta}\,\mu\,\hat{\eta}_{0\xi\xi} + \hat{\gamma}\,\mu\,\hat{\eta}_{0\xi\xi\xi\xi} = 0,$$

from which equation (2.8) is obtained. Equation (2.8) should be corrected as

$$\left[\hat{\eta}_{0\tau} + \hat{\epsilon}\,\hat{\eta}_0\,\hat{\eta}_{0\xi} + \frac{1}{2}\,\left(\hat{\delta} + \frac{1}{3}\right)\hat{\eta}_{0\xi\xi\xi} + \frac{\hat{\gamma}}{2}\,\hat{\eta}_{0\xi\xi\xi\xi\xi}\right]_\xi + \frac{\hat{\epsilon}}{2}\,\hat{\eta}_{0\zeta\zeta} = 0. \tag{9}$$

(2) Long water waves in the presence of surface tension. Let $m = 2$, $\delta = 0$, $\gamma = 0$, $\epsilon = \hat{\epsilon}\,\mu^2$, $\beta = \mu\,(1/3 - \alpha\,)$, $\alpha = \hat{\alpha}\,\mu$, and reference [5] obtains two equations between equations (2.8) and (2.9), which should be corrected as

$$-\hat{\eta}_{0\xi} - \mu\,\hat{\eta}_{1\xi} - \mu^2\,\hat{\eta}_{2\xi} + \mu^2\,\hat{\eta}_{0\tau} + \hat{\epsilon}\,\mu^2\,\hat{\eta}_{0\xi}\,\hat{\phi}_{0\xi} + \hat{\phi}_{0\xi\xi} + \mu\,\hat{\phi}_{1\xi\xi} + \mu^2\,\hat{\phi}_{2\xi\xi} + \hat{\epsilon}\,\mu^2\,\hat{\phi}_{0\zeta\zeta} + \frac{\mu}{3}\,\hat{\phi}_{0\xi\xi\xi\xi} + \frac{\mu^2}{3}\,\hat{\phi}_{1\xi\xi\xi\xi} + \frac{2\,\mu^2}{15}\,\hat{\phi}_{0\xi\xi\xi\xi} = 0,$$

$$-\hat{\phi}_{0\xi} - \mu\,\hat{\phi}_{1\xi} - \mu^2\,\hat{\phi}_{2\xi} + \mu^2\,\hat{\phi}_{0\tau} + \frac{\hat{\epsilon}\,\mu^2}{2}\,\hat{\phi}_{0\xi}^2 + \hat{\eta}_0 + \mu\,\hat{\eta}_1 + \mu^2\,\hat{\eta}_2 - \frac{\mu}{3}\,\hat{\eta}_{0\xi\xi} + \hat{\alpha}\,\mu^2\,\hat{\eta}_{0\xi\xi} - \frac{\mu^2}{3}\,\hat{\eta}_{1\xi\xi} = 0,$$

from which equation (2.9) is obtained. Equation (2.9) should be corrected as

$$\left[\hat{\eta}_{0\tau} + \hat{\epsilon}\,\hat{\eta}_0\,\hat{\eta}_{0\xi} + \frac{1}{2}\,\left(\hat{\alpha} + \frac{2}{15}\right)\hat{\eta}_{0\xi\xi\xi} - \frac{1}{9}\,\hat{\eta}_{0\xi\xi\xi\xi\xi}\right]_\xi + \hat{\epsilon}\,\hat{\eta}_{0\zeta\zeta} = 0. \tag{10}$$

Finally, equations (9) and (10) can be put in the form of equation (1) after scaling transformations.

3 Computerized symbolic computation and truncated Painlevé expansion

In this section, we will perform computerized symbolic computation with the truncated Painlevé expansion of the

$$\phi^{-10}:\ u_0 = -1680\,{\phi_x}^4\ , \tag{13}$$

$$\phi^{-9}:\ u_1 = 3360\,{\phi_x}^2\,\phi_{xx}, \tag{14}$$

$$\phi^{-8}:\ u_2 = \frac{-280\,s\,{\phi_x}^2}{13} - 840\,{\phi_{xx}}^2 - 1120\,\phi_x\,\phi_{xxx}, \tag{15}$$

$$\phi^{-7}:\ u_3 = \frac{280\,s\,\phi_{xx}}{13} + 280\,\phi_{xxxx}, \tag{16}$$

$$\begin{aligned}\phi^{-6}:\ & -507\,{\phi_y}^2\,{\phi_x}^2 - 507\,\phi_t\,{\phi_x}^3 + 31\,{\phi_x}^4 - 507\,u_4\,{\phi_x}^4 + 2730\,s\,{\phi_x}^2\,{\phi_{xx}}^2 + 53235\,{\phi_{xx}}^4\\ & -3640\,s\,{\phi_x}^3\,\phi_{xxx} - 141960\,\phi_x\,{\phi_{xx}}^2\,\phi_{xxx} + 70980\,{\phi_x}^2\,\phi_{xx}\,\phi_{xxxx}\\ & +47320\,{\phi_x}^2\,{\phi_{xxx}}^2 - 28392\,{\phi_x}^3\,\phi_{xxxxx} = 0,\end{aligned} \tag{17}$$

$$\begin{aligned}\phi^{-5}:\ & 507\,\phi_{yy}\,{\phi_x}^4 + 1014\,{\phi_x}^5\,u_{4,x} + 2535\,{\phi_x}^4\,\phi_{xt} + 4056\,\phi_y\,{\phi_x}^3\,\phi_{xy} + 3042\,{\phi_y}^2\,{\phi_x}^2\,\phi_{xx}\\ & +5070\,\phi_t\,{\phi_x}^3\,\phi_{xx} - 465\,{\phi_x}^4\,\phi_{xx} + 7605\,u_4\,{\phi_x}^4\,\phi_{xx} - 21840\,s\,{\phi_x}^2\,{\phi_{xx}}^3\\ & -53235\,{\phi_{xx}}^5 + 25480\,s\,{\phi_x}^3\,\phi_{xx}\,\phi_{xxx} + 473200\,{\phi_x}^2\,\phi_{xx}\,{\phi_{xxx}}^2\\ & +10010\,s\,{\phi_x}^4\,\phi_{xxxx} - 177450\,{\phi_x}^2\,{\phi_{xx}}^2\,\phi_{xxxx} - 473200\,{\phi_x}^3\,\phi_{xxx}\,\phi_{xxxx}\\ & +141960\,{\phi_x}^3\,\phi_{xx}\,\phi_{xxxxx} + 70980\,{\phi_x}^4\,\phi_{xxxxxx} = 0,\end{aligned} \tag{18}$$

$$\begin{aligned}\phi^{-4}:\ & -39\,s\,{\phi_y}^2\,{\phi_x}^2 - 39\,s\,\phi_t\,{\phi_x}^3 - 39\,s\,u_4\,{\phi_x}^4 - 6084\,{\phi_x}^2\,{\phi_{xy}}^2 - 2028\,{\phi_x}^3\,\phi_{xyy}\\ & -3042\,\phi_{yy}\,{\phi_x}^2\,\phi_{xx} - 10140\,{\phi_x}^3\,u_{4,x}\,\phi_{xx} - 15210\,{\phi_x}^2\,\phi_{xt}\,\phi_{xx}\\ & -12168\,\phi_y\,\phi_x\,\phi_{xy}\,\phi_{xx} - 1521\,{\phi_y}^2\,{\phi_{xx}}^2 - 7605\,\phi_t\,\phi_x\,{\phi_{xx}}^2 + 1605\,{\phi_x}^2\,{\phi_{xx}}^2\\ & -22815\,u_4\,{\phi_x}^2\,{\phi_{xx}}^2 + 13650\,s\,{\phi_{xx}}^4 - 507\,{\phi_x}^4\,u_{4,xx} - 5070\,{\phi_x}^3\,\phi_{xxt}\\ & -6084\,\phi_y\,{\phi_x}^2\,\phi_{xxy} - 2028\,{\phi_y}^2\,\phi_x\,\phi_{xxx} - 5070\,\phi_t\,{\phi_x}^2\,\phi_{xxx} + 340\,{\phi_x}^3\,\phi_{xxx}\\ & -10140\,u_4\,{\phi_x}^3\,\phi_{xxx} + 21840\,s\,\phi_x\,{\phi_{xx}}^2\,\phi_{xxx} - 32760\,s\,{\phi_x}^2\,{\phi_{xxx}}^2\\ & -118300\,{\phi_{xx}}^2\,{\phi_{xxx}}^2 - 473200\,\phi_x\,{\phi_{xxx}}^3 - 49140\,s\,{\phi_x}^2\,\phi_{xx}\,\phi_{xxxx}\\ & +177450\,{\phi_{xx}}^3\,\phi_{xxxx} + 236600\,\phi_x\,\phi_{xx}\,\phi_{xxx}\,\phi_{xxxx} + 502775\,{\phi_x}^2\,{\phi_{xxxx}}^2\\ & -12376\,s\,{\phi_x}^3\,\phi_{xxxxx} - 70980\,\phi_x\,{\phi_{xx}}^2\,\phi_{xxxxx} + 236600\,{\phi_x}^2\,\phi_{xxx}\,\phi_{xxxxx}\\ & -354900\,{\phi_x}^2\,\phi_{xx}\,\phi_{xxxxxx} - 60840\,{\phi_x}^3\,\phi_{xxxxxxx} = 0,\end{aligned} \tag{19}$$

$$\begin{aligned}\phi^{-3}:\ & 13\,s\,\phi_{yy}\,{\phi_x}^2 + 26\,s\,{\phi_x}^3\,u_{4,x} + 39\,s\,{\phi_x}^2\,\phi_{xt} + 52\,s\,\phi_y\,\phi_x\,\phi_{xy} + 13\,s\,{\phi_y}^2\,\phi_{xx}\\ & +39\,s\,\phi_t\,\phi_x\,\phi_{xx} + 78\,s\,u_4\,{\phi_x}^2\,\phi_{xx} + 2028\,{\phi_{xy}}^2\,\phi_{xx} + 2028\,\phi_x\,\phi_{xyy}\,\phi_{xx}\\ & +507\,\phi_{yy}\,{\phi_{xx}}^2 + 5070\,\phi_x\,u_{4,x}\,{\phi_{xx}}^2 + 2535\,\phi_{xt}\,{\phi_{xx}}^2 - 225\,{\phi_{xx}}^3\\ & +2535\,u_4\,{\phi_{xx}}^3 + 1014\,{\phi_x}^2\,\phi_{xx}\,u_{4,xx} + 5070\,\phi_x\,\phi_{xx}\,\phi_{xxt} + 4056\,\phi_x\,\phi_{xy}\,\phi_{xxy}\\ & +2028\,\phi_y\,\phi_{xx}\,\phi_{xxy} + 1014\,{\phi_x}^2\,\phi_{xxyy} + 676\,\phi_{yy}\,\phi_x\,\phi_{xxx} + 3380\,{\phi_x}^2\,u_{4,x}\,\phi_{xxx}\\ & +3380\,\phi_x\,\phi_{xt}\,\phi_{xxx} + 1352\,\phi_y\,\phi_{xy}\,\phi_{xxx} + 1690\,\phi_t\,\phi_{xx}\,\phi_{xxx} - 620\,\phi_x\,\phi_{xx}\,\phi_{xxx}\\ & +10140\,u_4\,\phi_x\,\phi_{xx}\,\phi_{xxx} - 3640\,s\,\phi_{xx}\,{\phi_{xxx}}^2 + 1690\,{\phi_x}^2\,\phi_{xxxt} + 55\,{\phi_x}^2\,\phi_{xxxx}\\ & +1352\,\phi_y\,\phi_x\,\phi_{xxxy} + 169\,{\phi_y}^2\,\phi_{xxxx} + 845\,\phi_t\,\phi_x\,\phi_{xxxx} + 2535\,u_4\,{\phi_x}^2\,\phi_{xxxx}\\ & +18200\,s\,\phi_x\,\phi_{xxx}\,\phi_{xxxx} + 118300\,{\phi_{xxx}}^2\,\phi_{xxxx} - 88725\,\phi_{xx}\,{\phi_{xxxx}}^2\\ & +8736\,s\,\phi_x\,\phi_{xx}\,\phi_{xxxxx} - 47320\,\phi_{xx}\,\phi_{xxx}\,\phi_{xxxxx} - 165620\,\phi_x\,\phi_{xxxx}\,\phi_{xxxxx}\\ & +3276\,s\,{\phi_x}^2\,\phi_{xxxxxx} + 35490\,{\phi_{xx}}^2\,\phi_{xxxxxx} + 47320\,\phi_x\,\phi_{xxx}\,\phi_{xxxxxx}\\ & +60840\,\phi_x\,\phi_{xx}\,\phi_{xxxxxxx} + 7605\,{\phi_x}^2\,\phi_{xxxxxxxx} = 0,\end{aligned} \tag{20}$$

dependent variable in a Laurent series about the pole manifold $\phi(x,y,t)=0$ in the sense of [13,16,20,23]:

$$u(x,y,t) = \phi(x,y,t)^{-J}\sum_{l=0}^{J} u_l(x,y,t)\,\phi(x,y,t)^l, \tag{11}$$

where $u_l(x,y,t)$ and $\phi(x,y,t)$ are both analytic functions with $u_0(x,y,t)\neq 0$ and $\phi_x(x,y,t)\neq 0$, while J is the natural number determined via the leading-order analysis as $J=4$, so that

$$u(x,y,t) = \phi(x,y,t)^{-4}\sum_{l=0}^{4} u_l(x,y,t)\,\phi(x,y,t)^l. \tag{12}$$

With symbolic computation, we substitute expression (12) into equation (1), make the coefficients of like powers of ϕ to vanish, and after manipulations, get the set of Painlevé-Bäcklund equations as follows:

see equations (13, 14, 15, 16, 17, 18, 19, 20) above and (21, 22, 23) in next pages.

4 Bäcklund transformation and format of solutions

What we have obtained is the set of equations (12–23), which constitutes an *auto-Bäcklund transformation*, since

$$\begin{aligned}
\phi^{-2}:\ & -26\,s\,{\phi_{xy}}^2-26\,s\,\phi_x\,\phi_{xyy}-13\,s\,\phi_{yy}\,\phi_{xx}-78\,s\,\phi_x\,u_{4,x}\,\phi_{xx}-39\,s\,\phi_{xt}\,\phi_{xx}\\
& -39\,s\,u_4\,{\phi_{xx}}^2-13\,s\,{\phi_x}^2\,u_{4,xx}-507\,{\phi_{xx}}^2\,u_{4,xx}-39\,s\,\phi_x\,\phi_{xxt}-1014\,{\phi_{xxy}}^2\\
& -26\,s\,\phi_y\,\phi_{xxy}-1014\,\phi_{xx}\,\phi_{xxyy}-13\,s\,\phi_t\,\phi_{xxx}-52\,s\,u_4\,\phi_x\,\phi_{xxx}\\
& -676\,\phi_{xyy}\,\phi_{xxx}-3380\,u_{4,x}\,\phi_{xx}\,\phi_{xxx}-676\,\phi_x\,u_{4,xx}\,\phi_{xxx}-1690\,\phi_{xxt}\,\phi_{xxx}\\
& +150\,{\phi_{xxx}}^2-1690\,u_4\,{\phi_{xxx}}^2-1690\,\phi_{xx}\,\phi_{xxxt}-1352\,\phi_{xy}\,\phi_{xxxy}\\
& -676\,\phi_x\,\phi_{xxxyy}-169\,\phi_{yy}\,\phi_{xxxx}-1690\,\phi_x\,u_{4,x}\,\phi_{xxxx}-845\,\phi_{xt}\,\phi_{xxxx}\\
& +85\,\phi_{xx}\,\phi_{xxxx}-2535\,u_4\,\phi_{xx}\,\phi_{xxxx}-2730\,s\,{\phi_{xxx}}^2-845\,\phi_x\,\phi_{xxxxt}\\
& -338\,\phi_y\,\phi_{xxxxy}-169\,\phi_t\,\phi_{xxxxx}-78\,\phi_x\,\phi_{xxxxx}-1014\,u_4\,\phi_x\,\phi_{xxxxx}\\
& -2912\,s\,\phi_{xxx}\,\phi_{xxxxx}+26026\,{\phi_{xxxxx}}^2-1456\,s\,\phi_{xx}\,\phi_{xxxxxx}\\
& +11830\,\phi_{xxxx}\,\phi_{xxxxxx}-1456\,s\,\phi_x\,\phi_{xxxxxxx}-20280\,\phi_{xxx}\,\phi_{xxxxxxx}\\
& -7605\,\phi_{xx}\,\phi_{xxxxxxxx}-1690\,\phi_x\,\phi_{xxxxxxxxx}=0, \qquad (21)\\
\phi^{-1}:\ & s\,\phi_{xx}\,u_{4,xx}+s\,\phi_{xxyy}+2\,s\,u_{4,x}\,\phi_{xxx}+s\,\phi_{xxxt}+s\,u_4\,\phi_{xxxx}+13\,u_{4,xx}\,\phi_{xxxx}\\
& +13\,\phi_{xxxxyy}+26\,u_{4,x}\,\phi_{xxxxx}+13\,\phi_{xxxxxt}+\phi_{xxxxxx}+13\,u_4\,\phi_{xxxxxx}\\
& +14\,s\,\phi_{xxxxxxxx}+13\,\phi_{xxxxxxxxxx}=0, \qquad (22)\\
\phi^{0}:\ & u_{4,xt}+\left(u_4\,u_{4,x}\right)_x+s\,u_{4,xxxx}+u_{4,xxxxxx}+u_{4,yy}=0. \qquad (23)
\end{aligned}$$

$$\begin{aligned}
u(x,y,t)=\ & \frac{280\,\alpha^2\,e^{\alpha\,x+y\,\beta(t)+\gamma(t)}\,\left(13\,\alpha^2+s\right)}{13\,\left[1+e^{\alpha\,x+y\,\beta(t)+\gamma(t)}\right]}-\frac{280\,\alpha^2\,e^{2\,\alpha\,x+2\,y\,\beta(t)+2\,\gamma(t)}\,\left(91\,\alpha^2+s\right)}{13\,\left[1+e^{\alpha\,x+y\,\beta(t)+\gamma(t)}\right]^2}\\
& +\frac{3360\,\alpha^4\,e^{3\,\alpha\,x+3\,y\,\beta(t)+3\,\gamma(t)}}{\left[1+e^{\alpha\,x+y\,\beta(t)+\gamma(t)}\right]^3}-\frac{1680\,\alpha^4\,e^{4\,\alpha\,x+4\,y\,\beta(t)+4\,\gamma(t)}}{\left[1+e^{\alpha\,x+y\,\beta(t)+\gamma(t)}\right]^4}\\
& +\frac{31}{507}+\frac{7\,\alpha^4}{3}-\frac{70\,\alpha^2\,s}{39}-\frac{\beta(t)^2}{\alpha^2}-\frac{y\,\beta'(t)}{\alpha}-\frac{\gamma'(t)}{\alpha}\\
=\ & \frac{31}{507}-\frac{98\,\alpha^4}{3}+\frac{140\,\alpha^2\,s}{39}-\frac{\beta(t)^2}{\alpha^2}-105\,\alpha^4\,\mathrm{Tanh}^4\left[\frac{\alpha\,x+y\,\beta(t)+\gamma(t)}{2}\right]\\
& +\frac{70\,\alpha^2\,\left(26\,\alpha^2-s\right)}{13}\,\mathrm{Tanh}^2\left[\frac{\alpha\,x+y\,\beta(t)+\gamma(t)}{2}\right]-\frac{y\,\beta'(t)}{\alpha}-\frac{\gamma'(t)}{\alpha}, \qquad (29)
\end{aligned}$$

the whole set is mutually consistent, or, explicitly solvable with respect to $\phi(x,y,t)$, $u_0(x,y,t)$, $u_1(x,y,t)$, $u_2(x,y,t)$, $u_3(x,y,t)$ and $u_4(x,y,t)$. Solvable examples are as below:

For the solitonic features, we begin to construct a trial solution,

$$\phi(x,y,t)=1+e^{x\,\alpha(t)+y\,\beta(t)+\gamma(t)}, \qquad (24)$$

where the functions $\alpha(t)$, $\beta(t)$ and $\gamma(t)$ are sufficiently differentiable, with $\alpha(t)\neq 0$ since $\phi_x\neq 0$. The x- and y-linear form is used solely for the simplification of the computation work. Using expression (24), we perform symbolic computation, and get

$$\begin{aligned}
\phi^{-6}:\ & u_4(x,y,t)=\frac{31}{507}+\frac{7\,\alpha(t)^4}{3}\\
& -\frac{70\,\alpha(t)^2\,s}{39}-\frac{\beta(t)^2}{\alpha(t)^2}-\frac{y\,\beta'(t)}{\alpha(t)}-\frac{\gamma'(t)}{\alpha(t)}, \qquad (25)\\
\phi^{-5}:\ & \alpha'(t)=0 \qquad \Rightarrow \qquad \alpha=\mathrm{const}. \qquad (26)\\
\phi^{0}:\ & \text{satisfied}. \qquad (27)
\end{aligned}$$

Then, the coefficients of ϕ^{-4}, ϕ^{-3}, ϕ^{-2} and ϕ^{-1} give rise to the same equation,

$$\phi^{-4},\ \phi^{-3},\ \phi^{-2}\quad \phi^{-1}:\ 21970\,\alpha^6+31\,s-3549\,\alpha^4\,s=0. \qquad (28)$$

With the relevant expressions combined together, we in fact arrive at a *format of exact analytic solutions* to equation (1), as follows,

see equation (29) above

in which the constant α needs to satisfy constraint (28).

With the travelling-wave assumptions, i.e., $\gamma(t)=\gamma_1\,t+\gamma_2$, while β, γ_1 and γ_2 are constants, the aforementioned set of Bäcklund transformation turns out to be a system of algebraic polynomial equations. We can make use of the Wu elimination method, which is a very sufficient method to solve for the systems of algebraic polynomial equations with many unknowns [24–26], along with symbolic computation, to get the solitary-wave solutions to equation (1), which are pictured out in Figures 1 and 6, and are in fact a special case of format (29).

$$
\begin{aligned}
u_I^{\sigma}(x,y,t) =& \frac{31}{507}+\frac{14\,s}{507}\left[\left(-120\sqrt{93}-1207\,s\right)^{\frac{1}{3}}+\left(120\sqrt{93}-1207\,s\right)^{\frac{1}{3}}+7\,s\right]\\
&-\frac{49}{25350}\left[\left(-120\sqrt{93}-1207\,s\right)^{\frac{1}{3}}+\left(120\sqrt{93}-1207\,s\right)^{\frac{1}{3}}+7\,s\right]^2\\
&-\frac{130\,\beta(t)^2}{\left(-120\sqrt{93}-1207\,s\right)^{\frac{1}{3}}+\left(120\sqrt{93}-1207\,s\right)^{\frac{1}{3}}+7\,s}\\
&+\frac{7}{169}\left[\left(-120\sqrt{93}-1207\,s\right)^{\frac{1}{3}}+\left(120\sqrt{93}-1207\,s\right)^{\frac{1}{3}}+7\,s\right]\\
&\times\left[-s+\frac{\left(-120\sqrt{93}-1207\,s\right)^{\frac{1}{3}}+\left(120\sqrt{93}-1207\,s\right)^{\frac{1}{3}}+7\,s}{5}\right]\\
&\times\tanh^2\left[\frac{\frac{\sigma\sqrt{\left(-120\sqrt{93}-1207\,s\right)^{\frac{1}{3}}+\left(120\sqrt{93}-1207\,s\right)^{\frac{1}{3}}+7\,s}}{\sqrt{130}}\,x+y\,\beta(t)+\gamma(t)}{2}\right]\\
&-\frac{21}{3380}\left[\left(-120\sqrt{93}-1207\,s\right)^{\frac{1}{3}}+\left(120\sqrt{93}-1207\,s\right)^{\frac{1}{3}}+7\,s\right]^2\\
&\times\tanh^4\left[\frac{\frac{\sigma\sqrt{\left(-120\sqrt{93}-1207\,s\right)^{\frac{1}{3}}+\left(120\sqrt{93}-1207\,s\right)^{\frac{1}{3}}+7\,s}}{\sqrt{130}}\,x+y\,\beta(t)+\gamma(t)}{2}\right]\\
&-\frac{\sqrt{130}\,\sigma\,y\,\beta'(t)}{\sqrt{\left(-120\sqrt{93}-1207\,s\right)^{\frac{1}{3}}+\left(120\sqrt{93}-1207\,s\right)^{\frac{1}{3}}+7\,s}}\\
&-\frac{\sqrt{130}\,\sigma\,\gamma'(t)}{\sqrt{\left(-120\sqrt{93}-1207\,s\right)^{\frac{1}{3}}+\left(120\sqrt{93}-1207\,s\right)^{\frac{1}{3}}+7\,s}}. \qquad (35)
\end{aligned}
$$

5 Families of exact analytic solutions

By virtue of the transformation

$$\alpha^2=\Psi+\frac{7\,s}{130}. \qquad (30)$$

Constraint (28) becomes

$$\Psi^3-\frac{147\,\Psi}{16900}+\frac{1207\,s}{1098500}=0. \qquad (31)$$

Make use of the Cardan formulae (as seen, e.g., in Ref. [27]), and we find 3 roots for Ψ, as below. For each root Ψ_n, we have

$$\alpha_n^{\sigma}=\sigma\sqrt{\Psi_n+\frac{7\,s}{130}}\qquad\text{with}\qquad\sigma=\pm1\qquad\text{and}\qquad n=I,II,III. \qquad (32)$$

Type I: Family I-a and Family I-b

For

$$\Psi_I=\frac{\left(-120\sqrt{93}-1207\,s\right)^{\frac{1}{3}}+\left(120\sqrt{93}-1207\,s\right)^{\frac{1}{3}}}{130}, \qquad (39)$$

or

$$\alpha_I^{\sigma}=\frac{\sigma\sqrt{\left(-120\sqrt{93}-1207\,s\right)^{\frac{1}{3}}+\left(120\sqrt{93}-1207\,s\right)^{\frac{1}{3}}+7\,s}}{\sqrt{130}}. \qquad (40)$$

Format (29) gives rise to *the first type of exact analytic solutions* to equation (1), as follows,

see equation (35) above.

There exist 2 families of solutions in Type I, named as Family I-a and Family I-b, for $\sigma=\pm1$ separately.

For $s=-1$, real $\beta(t)$ and real $\gamma(t)$, Type I becomes *solitonic*, which is of special interest and going to be discussed later.

Type II: Family II-a and Family II-b

For

$$\Psi_{II}=\frac{\left(-1-i\sqrt{3}\right)\left(-120\sqrt{93}-1207\,s\right)^{\frac{1}{3}}}{260}+\frac{\left(-1+i\sqrt{3}\right)\left(120\sqrt{93}-1207\,s\right)^{\frac{1}{3}}}{260}, \qquad (36)$$

or

$$\alpha_{II}^{\sigma}=\sigma\sqrt{\frac{\left(-1-i\sqrt{3}\right)\,\left(-120\sqrt{93}-1207\,s\right)^{\frac{1}{3}}}{260}+\frac{\left(-1+i\sqrt{3}\right)\,\left(120\sqrt{93}-1207\,s\right)^{\frac{1}{3}}}{260}+\frac{7\,s}{130}}, \tag{37}$$

$$\begin{aligned}u_{II}^{\sigma}(x,y,t)=&\frac{31}{507}-\frac{98\left[\frac{\left(-1-i\sqrt{3}\right)\left(-120\sqrt{93}-1207\,s\right)^{\frac{1}{3}}}{260}+\frac{\left(-1+i\sqrt{3}\right)\left(120\sqrt{93}-1207\,s\right)^{\frac{1}{3}}}{260}+\frac{7\,s}{130}\right]^{2}}{3}\\&+\frac{140\left[\frac{\left(-1-i\sqrt{3}\right)\left(-120\sqrt{93}-1207\,s\right)^{\frac{1}{3}}}{260}+\frac{\left(-1+i\sqrt{3}\right)\left(120\sqrt{93}-1207\,s\right)^{\frac{1}{3}}}{260}+\frac{7\,s}{130}\right]s}{39}\\&-\frac{\beta(t)^{2}}{\frac{\left(-1-i\sqrt{3}\right)\left(-120\sqrt{93}-1207\,s\right)^{\frac{1}{3}}}{260}+\frac{\left(-1+i\sqrt{3}\right)\left(120\sqrt{93}-1207\,s\right)^{\frac{1}{3}}}{260}+\frac{7\,s}{130}}\\&+\frac{70\left\{26\left[\frac{\left(-1-i\sqrt{3}\right)\left(-120\sqrt{93}-1207\,s\right)^{\frac{1}{3}}}{260}+\frac{\left(-1+i\sqrt{3}\right)\left(120\sqrt{93}-1207\,s\right)^{\frac{1}{3}}}{260}+\frac{7\,s}{130}\right]-s\right\}}{13}\\&\times\left[\frac{\left(-1-i\sqrt{3}\right)\,\left(-120\sqrt{93}-1207\,s\right)^{\frac{1}{3}}}{260}+\frac{\left(-1+i\sqrt{3}\right)\,\left(120\sqrt{93}-1207\,s\right)^{\frac{1}{3}}}{260}+\frac{7\,s}{130}\right]\\&\times\mathrm{Tanh}^{2}\left[\frac{\sigma\sqrt{\frac{\left(-1-i\sqrt{3}\right)\left(-120\sqrt{93}-1207\,s\right)^{\frac{1}{3}}}{260}+\frac{\left(-1+i\sqrt{3}\right)\left(120\sqrt{93}-1207\,s\right)^{\frac{1}{3}}}{260}+\frac{7\,s}{130}}\,x+y\,\beta(t)+\gamma(t)}{2}\right]\\&-105\left[\frac{\left(-1-i\sqrt{3}\right)\,\left(-120\sqrt{93}-1207\,s\right)^{\frac{1}{3}}}{260}+\frac{\left(-1+i\sqrt{3}\right)\,\left(120\sqrt{93}-1207\,s\right)^{\frac{1}{3}}}{260}+\frac{7\,s}{130}\right]^{2}\\&\times\mathrm{Tanh}^{4}\left[\frac{\sigma\sqrt{\frac{\left(-1-i\sqrt{3}\right)\left(-120\sqrt{93}-1207\,s\right)^{\frac{1}{3}}}{260}+\frac{\left(-1+i\sqrt{3}\right)\left(120\sqrt{93}-1207\,s\right)^{\frac{1}{3}}}{260}+\frac{7\,s}{130}}\,x+y\,\beta(t)+\gamma(t)}{2}\right]\\&-\frac{\sigma\,y\,\beta'(t)}{\sqrt{\frac{\left(-1-i\sqrt{3}\right)\left(-120\sqrt{93}-1207\,s\right)^{\frac{1}{3}}}{260}+\frac{\left(-1+i\sqrt{3}\right)\left(120\sqrt{93}-1207\,s\right)^{\frac{1}{3}}}{260}+\frac{7\,s}{130}}}\\&-\frac{\sigma\,\gamma'(t)}{\sqrt{\frac{\left(-1-i\sqrt{3}\right)\left(-120\sqrt{93}-1207\,s\right)^{\frac{1}{3}}}{260}+\frac{\left(-1+i\sqrt{3}\right)\left(120\sqrt{93}-1207\,s\right)^{\frac{1}{3}}}{260}+\frac{7\,s}{130}}}.\end{aligned} \tag{38}$$

see equation (37) above.

Format (29) gives rise to *the second type of exact analytic solutions* to equation (1),

see equation (38) above.

There exist 2 families of solutions in this type, named as Family II-a and Family II-b, for $\sigma=\pm1$ separately.

Type III: Family III-a and Family III-b

For

$$\Psi_{III}=\frac{\left(-1+i\sqrt{3}\right)\,\left(-120\sqrt{93}-1207\,s\right)^{\frac{1}{3}}}{260}+\frac{\left(-1-i\sqrt{3}\right)\,\left(120\sqrt{93}-1207\,s\right)^{\frac{1}{3}}}{260}, \tag{39}$$

or

see equation (40) in next page.

Format (29) gives rise to *the third type of exact analytic solutions* to equation (1),

see equation (41) in next page.

There exist 2 families of solutions in this type, named as Family III-a and Family III-b, for $\sigma=\pm1$ separately.

Altogether, we can find 3 types, or 6 families, of the exact analytic solutions for equation (1).

6 Discussions

Of special interest are the *solitonic* solutions from Type I, for $s=-1$, real $\beta(t)$ and $\gamma(t)$, which has been considered in our previous work, i.e., reference [21], to some extent. This interesting case deserves more detailed discussions,

$$\alpha^{\sigma}_{III}=\sigma\sqrt{\frac{\left(-1+i\sqrt{3}\right)\left(-120\sqrt{93}-1207\,s\right)^{\frac{1}{3}}}{260}+\frac{\left(-1-i\sqrt{3}\right)\left(120\sqrt{93}-1207\,s\right)^{\frac{1}{3}}}{260}+\frac{7\,s}{130}}, \tag{40}$$

$$\begin{aligned}u^{\sigma}_{III}(x,y,t)=&\frac{31}{507}-\frac{98\left[\frac{\left(-1+i\sqrt{3}\right)\left(-120\sqrt{93}-1207\,s\right)^{\frac{1}{3}}}{260}+\frac{\left(-1-i\sqrt{3}\right)\left(120\sqrt{93}-1207\,s\right)^{\frac{1}{3}}}{260}+\frac{7\,s}{130}\right]^2}{3}\\&+\frac{140\left[\frac{\left(-1+i\sqrt{3}\right)\left(-120\sqrt{93}-1207\,s\right)^{\frac{1}{3}}}{260}+\frac{\left(-1-i\sqrt{3}\right)\left(120\sqrt{93}-1207\,s\right)^{\frac{1}{3}}}{260}+\frac{7\,s}{130}\right]s}{39}\\&-\frac{\beta(t)^2}{\frac{\left(-1+i\sqrt{3}\right)\left(-120\sqrt{93}-1207\,s\right)^{\frac{1}{3}}}{260}+\frac{\left(-1-i\sqrt{3}\right)\left(120\sqrt{93}-1207\,s\right)^{\frac{1}{3}}}{260}+\frac{7\,s}{130}}\\&+\frac{70\left\{26\left[\frac{\left(-1+i\sqrt{3}\right)\left(-120\sqrt{93}-1207\,s\right)^{\frac{1}{3}}}{260}+\frac{\left(-1-i\sqrt{3}\right)\left(120\sqrt{93}-1207\,s\right)^{\frac{1}{3}}}{260}+\frac{7\,s}{130}\right]-s\right\}}{13}\\&\times\left[\frac{\left(-1+i\sqrt{3}\right)\left(-120\sqrt{93}-1207\,s\right)^{\frac{1}{3}}}{260}+\frac{\left(-1-i\sqrt{3}\right)\left(120\sqrt{93}-1207\,s\right)^{\frac{1}{3}}}{260}+\frac{7\,s}{130}\right]\\&\times\mathrm{Tanh}^2\left[\frac{\sigma\sqrt{\frac{\left(-1+i\sqrt{3}\right)\left(-120\sqrt{93}-1207\,s\right)^{\frac{1}{3}}}{260}+\frac{\left(-1-i\sqrt{3}\right)\left(120\sqrt{93}-1207\,s\right)^{\frac{1}{3}}}{260}+\frac{7\,s}{130}}\,x+y\,\beta(t)+\gamma(t)}{2}\right]\\&-105\left[\frac{\left(-1+i\sqrt{3}\right)\left(-120\sqrt{93}-1207\,s\right)^{\frac{1}{3}}}{260}+\frac{\left(-1-i\sqrt{3}\right)\left(120\sqrt{93}-1207\,s\right)^{\frac{1}{3}}}{260}+\frac{7\,s}{130}\right]^2\\&\times\mathrm{Tanh}^4\left[\frac{\sigma\sqrt{\frac{\left(-1+i\sqrt{3}\right)\left(-120\sqrt{93}-1207\,s\right)^{\frac{1}{3}}}{260}+\frac{\left(-1-i\sqrt{3}\right)\left(120\sqrt{93}-1207\,s\right)^{\frac{1}{3}}}{260}+\frac{7\,s}{130}}\,x+y\,\beta(t)+\gamma(t)}{2}\right]\\&-\frac{\sigma\,y\,\beta'(t)}{\sqrt{\frac{\left(-1+i\sqrt{3}\right)\left(-120\sqrt{93}-1207\,s\right)^{\frac{1}{3}}}{260}+\frac{\left(-1-i\sqrt{3}\right)\left(120\sqrt{93}-1207\,s\right)^{\frac{1}{3}}}{260}+\frac{7\,s}{130}}}\\&-\frac{\sigma\,\gamma'(t)}{\sqrt{\frac{\left(-1+i\sqrt{3}\right)\left(-120\sqrt{93}-1207\,s\right)^{\frac{1}{3}}}{260}+\frac{\left(-1-i\sqrt{3}\right)\left(120\sqrt{93}-1207\,s\right)^{\frac{1}{3}}}{260}+\frac{7\,s}{130}}}.\end{aligned} \tag{41}$$

as follows, with all the figures plotted with the vertical direction as $-u(x,y,t)$ for a clear viewpoint:

1. Equation (1) for $s=-1$ holds for the waves in the presence of large surface tension, when the dimensionless Bond number B_o ia larger than, but has to be close to, B_o^*, where the critical value $B_o^*=1/3$, while the Bond number $B_o=T/(\rho_w\,g\,H^2)$ (see Refs. [5,6,8] for details), where T is the value of surface tension, ρ_w is the liquid density, g is the acceleration of gravitation, and H is the liquid depth.
2. The auto-Bäcklund transformation, or the set of equations (12–23), works as a system of equations relating a "seed" solution of equation (1) to another (more complicated) solution of equation (1) itself. This way we would, in principle at least, be able to progressively construct more and more complicated solutions of equation (1). For example, if the seed is the solitonic expression (35), we could construct more complicated "solitonic" solutions of equation (1).
3. Figure 1, the same as the first plot in our paper [21], provides us with a solitary-wave picture for Family I-a in expression (35) taken at a fixed time, the specific look at which with different values of y is given in Figure 2.
4. Compared with Figure 1, we see that Figure 3 indicates that the transverse influence varies as β changes, Figure 4 shows the propagation of the wave as time goes on, and Figure 5 reverses the sign of σ for Family I-b. Please note that the values chosen for the free parameters and functions occurring in the solitonic solutions. are purely for the purpose of picture drawing and qualitative analysis. In reality, the detailed application of the solitonic solutions requires a judicious choice of those parameters and functions.

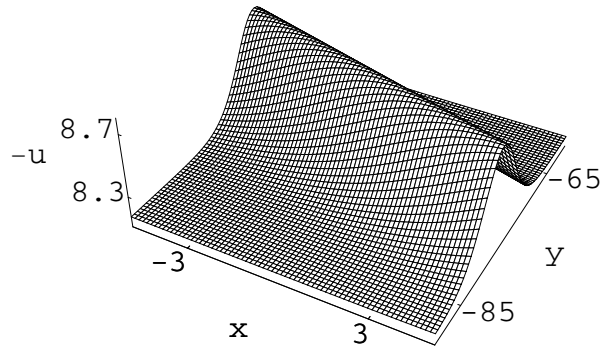

Fig. 1. Observable solution surface $u(x, y, t)$ of equation (1) describing a solitary wave via Family I-a in expression (35), with the parameters chosen as $s = -1$, $\sigma = 1$, $\beta(t) = 0.3$, $\gamma(t) = 2\,t + 2$, and then, $t = 0$. This is a photograph taken at a fixed time.

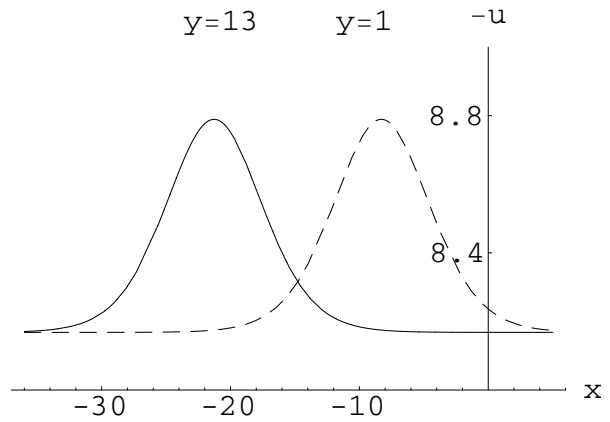

Fig. 2. Specific look at Figure 1, with two different values of y.

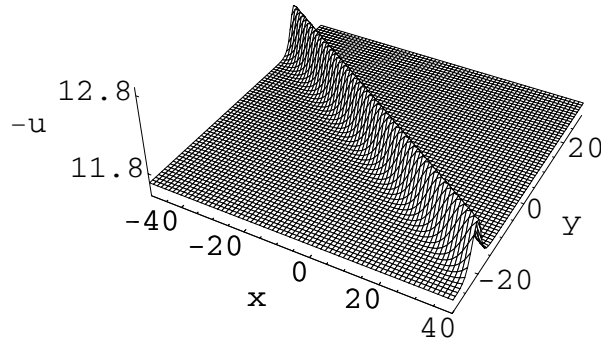

Fig. 3. $u(x, y, t)$ via expression (35), the same as Figure 1 except that $\beta = 0.6$ with the transverse influence changing.

5. As shown in Figures 1, 3, 4 and 5, the transverse influences can be characterized by the $x \sim y$ slopes on the wave positions. Figure 2 further illustrates this feature: A slope implies that at the *same* time, two observers at *different* $y_1(= 1)$ and $y_2(= 13)$ are able to see the wave locating at *different* $x_1(\simeq -8)$ and $x_2(\simeq -21)$. Hopefully, future experiments could investigate such a *two-dimensional, possibly observable* effect.
6. Along the propagation direction and for a fixed transverse position $y(= 0)$, Figures 7 and 8 picture out expression (35), the soliton-like solutions to equation (1),

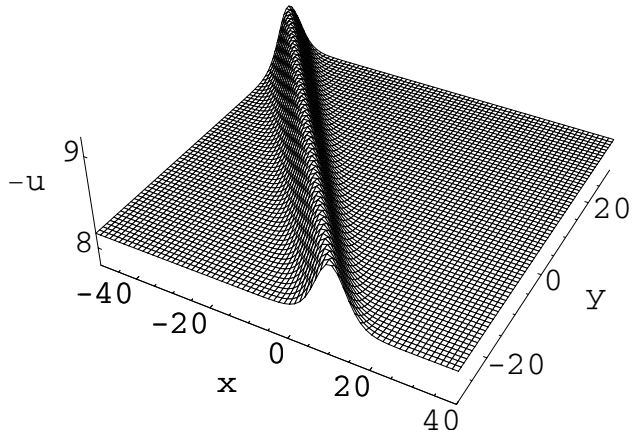

Fig. 4. $u(x, y, t)$ via expression (35) with $t = 2$, i.e., another picture taken at a different time. Other values remain the same as in Figure 1.

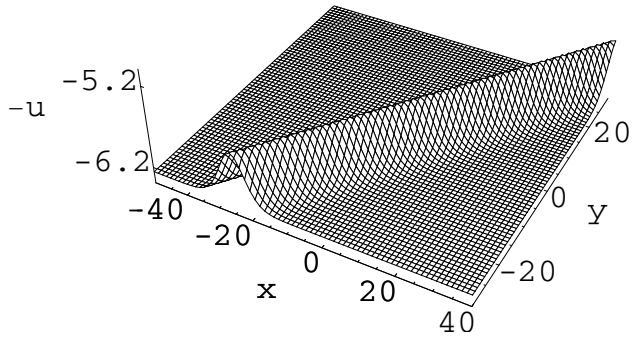

Fig. 5. $u(x, y, t)$ in expression (35) with $\sigma = -1$, showing Family I-b. The rest will be the same as Figure 1.

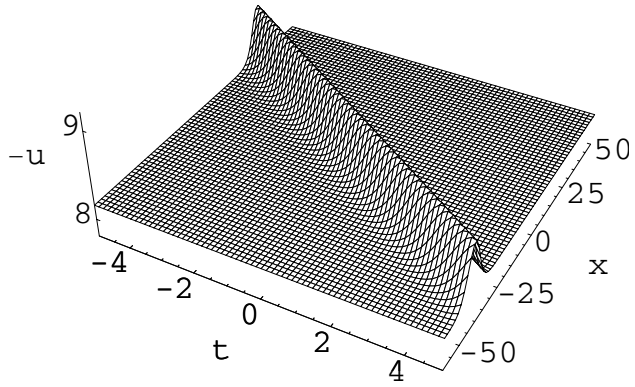

Fig. 6. The same as Figure 1 except that t varies but y is fixed as zero. This is a travelling-wave picture, for Figures 7 and 8 to be compared with.

with different non-travelling-wave functions assumed. The travelling-wave-natured Figure 6 is presented for the comparison purpose. Figures 7 and 8 address that the situation along the *propagation direction* could be fairly complicated beyond the travelling waves, resulting in the *non-constant vertical shifts* of the waves. The effect is also *possibly observable* with the future experiments. Figures 7 and 8 are the same as the second and third plots in our paper [21].

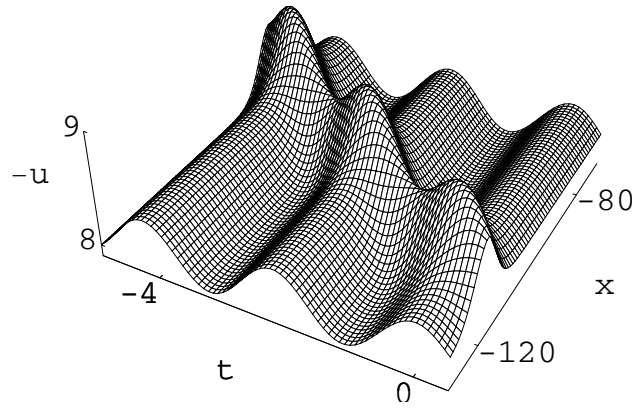

Fig. 7. Observable soliton-like solution surface $u(x, y, t)$ of equation (1) via expression (35). The parameters are the same as those in Figure 6 except that $\gamma(t) = 2\,t + 2 + Sin\,(3\,t)\,/50$.

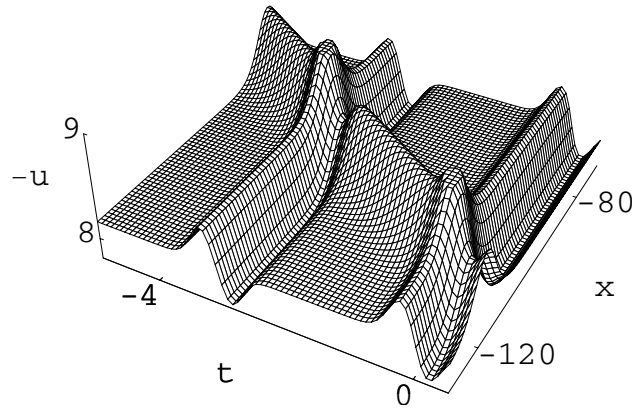

Fig. 8. The same as Figure 7 except that $\gamma(t) = 2\,t + 2 + \frac{1}{30}\left[\sum_{n=-\infty}^{\infty} e^{-10\,(t+3\,n)^2}\right]$.

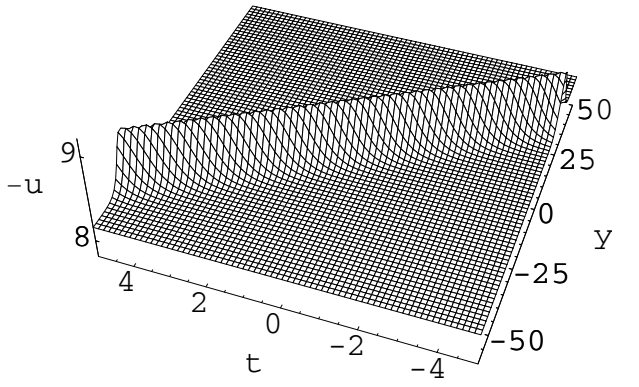

Fig. 9. The same as Figure 6 except that y changes with $x = 0$ fixed, which is a travelling-wave picture for Figures 10 and 11 to be compared with.

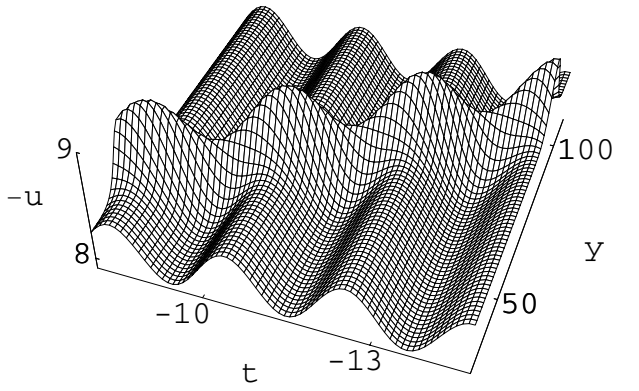

Fig. 10. Observable soliton-like solution surface $u(x, y, t)$ of equation (1) via expression (35), with the fixed $x = 0$ and changeable y. The rest will be the same as Figure 7.

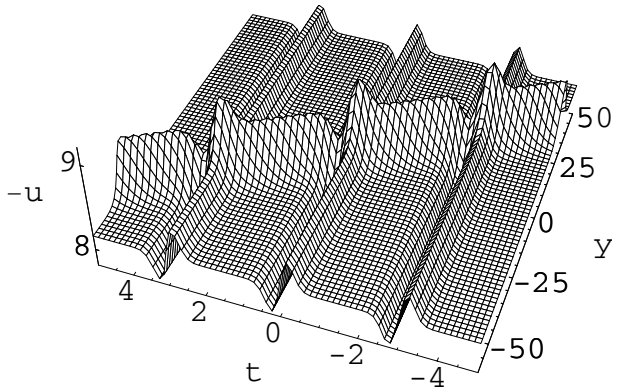

Fig. 11. Observable soliton-like solution surface $u(x, y, t)$ of equation (1) via expression (35), with the fixed $x = 0$ and changeable y. The rest will be the same as Figure 8.

7. On the other hand, along the transverse direction and with a fixed $x(= 0)$, Figures 10 and 11 deal with expression (35) as well, with different non-travelling-wave functions assigned. Figure 9 works here as a travelling-wave picture for the comparison purpose. Figures 10 and 11 make clear that the situation along the *transverse direction* could also be complicated beyond the travelling waves, resulting in the *non-constant vertical shifts* of the waves. Those effects *might be observable* with the future experiments as well. Again, an one-dimensional observation will *not* work. Figure 10 is the same as the fourth plot in our paper [21].
8. From the *open* sea, i.e., without any influence of the y- boundary conditions, as observed in St. Anthony Bight, Newfoundland and reported in reference [2], the incoming sea waves incident on the ice edge cause the break-up of the seemingly robust fast ice in only several hours. Especially, as shown in Figure 1 of reference [2], the cracking of shore-fast ice, somehow, occurs at uniform intervals, resulting in the formation of floating strips of approximately equal width.
   This ice-damage observation *might be explained* with the help of our solutions. As seen in Figures 7, 8, 10 and 11, the non-constant vertical shifts of the waves could be periodic when the arbitrary function $\gamma(t)$ is chosen to incorporate a periodic feature. Thus, mathematically allowed by equation (1), and physically incident from open water and normal to the ice edge, the periodic waves in Figures 7, 8, 10 and 11 have their crests/troughs located at an approximately equal distance from each other. It has been claimed [3,4] that the high curvatures and pressures developed near the

wave crests and troughs, propagating under the elastic ice sheet, cause cracking to occur, resulting in the formation of floating blocks of ice.

Thus, there appears the *possibility* that we have presented a way to explain the parallel cracks in ice, which also have uniform intervals. The differences between our possibility and those proposed in references [5, 6] are: (1) Ours do not rely on any boundary conditions, especially none in the y direction, which is in agreement with the *open* sea observations reported in reference [2]. (2) Ours are the exact solutions, not approximate. (3) Ours go beyond the travelling solitary waves.

7 Conclusions

The studies on the liquid surfaces for oceans, rivers, liquid propellant for rockets, aviation kerosene etc., are of current interest.

In this paper, we have investigated the (2+1) dimensional Hărăgus-Courcelle-Il'ichev model for the liquid surface waves in the presence of sea ice or surface tension. Our results are as follows:

- We have corrected some errors in the original derivations of this model;
- We have performed the computerized symbolic computation and truncated Painlevé expansion to obtain an auto-Bäcklund transformation for this model;
- We have performed the computerized symbolic computation with auto-Bäcklund transformation to obtain three types of the solitonic and other exact analytic solutions to this model, with the solitary waves as a special case;
- We have discussed the above results, with 11 figures presented;
- We have proposed certain possibly observable effects for the future experiments;
- We have provided a possibility to explain the regular structure of the sea ice break-up observations.

We express our sincere thanks to Editor Bohr and the Referee for their valuable comments. This work has been supported by the Excellent Young Teachers Program of the Ministry of Education of China, by the National Natural Science Foundation of China under Grants No. 10272017 and 60372095, by the National Key Basic Research Special Foundation (NKBRSF) of China under Grant No. G1999032701, by the W.T. Wu Foundation on Mathematics Mechanization, by the Talent Construction Special Fund of Beijing University of Aeronautics and Astronautics, by the Discipline Construction Grant BHB985-1-7 of Beijing University of Aeronautics and Astronautics under the Action Plan for the Revitalization of Education in the 21st Century of the Ministry of Education of China. BT also thanks the Enterprise Chair Professors Programme of Beijing University of Posts and Telecommunications and the Bright Oceans Corporation. YTG would like to acknowledge the Cheung Kong Scholars Programme of the Ministry of Education of China and Li Ka Shing Foundation of Hong Kong.

References

1. A. Müller, B. Ettema, Proc. IAHR Ice Symp., Hamburg, **II**, 287 (1992)
2. V. Squire, Cold Reg. Sci. Tech. **10**, 59 (1984)
3. L. Forbes, J. Fluid Mech. **169**, 409 (1986)
4. L. Forbes, J. Fluid Mech. **188**, 491 (1988)
5. M. Hărăgus-Courcelle, A. Il'ichev, Eur. J. Mech. B **17**, 739 (1998)
6. A. Il'ichev, Eur. J. Mech. B **18**, 501 (1999)
7. A. Il'ichev, Fluid Dynamics **35**, 157 (2000)
8. I. Bakholdin, A. Il'ichev, Eur. J. Mech. B **22**, 291 (2003)
9. T. Benjamin, Q. Appl. Math. **40**, 231 (1982)
10. G. Iooss, K. Kirchgässner, C.R. Acad. Sci. Paris **311**, 265 (1990)
11. G. Iooss, K. Kirchgässner, Proc. Roy. Soc. Edinburgh A **122**, 267 (1992)
12. A. Il'ichev, K. Kirchgässner, Universität Stutgart, Bericht 98/19 SFB 404 (1998)
13. M. Coffey, Phys. Rev. B **54**, 1279 (1996)
14. B. Tian, Y.T. Gao, Computers Math. Applic. **31**, 115 (1996)
15. Y.T. Gao, B. Tian, Acta Mechanica **128**, 137 (1998)
16. W. Hong, Y. Jung, Phys. Lett. A **257**, 149 (1999)
17. B. Tian, Int. J. Mod. Phys. C **10**, 1089 (1999)
18. G. Das, J. Sarma, Phys. Plasmas **6**, 4394 (1999)
19. W. Hong, Y. Jung, Z. Naturforsch. A **54**, 272 (1999)
20. W. Hong, Y. Jung, Z. Naturforsch. A **54**, 549 (1999)
21. B. Tian, Y.T. Gao, Int. J. Mod. Phys. C **15**, 545 (2004)
22. M.P. Barnett, J.F. Capitani, J. Von Zur Gathen, J. Gerhard, Int. J. Quantum Chem. **100**, 80 (2004); Sirendaoreji, J. Phys. A **32**, 6897 (1999); W.P. Hong, S.H. Park, Int. J. Mod. Phys. C **15**, 363 (2004); F.D. Xie, X.S. Gao, Comm. Theor. Phys. **41**, 353 (2004); B. Li, Y. Chen, H.N. Xuan, H.Q. Zhang, Appl. Math. Comput. **152**, 581 (2004); Y.T. Gao, B. Tian, Phys. Plasmas **10**, 4306 (2003); B. Tian, Y.T. Gao, Nuov. Cim. B **118**, 175 (2003); B. Tian, Y.T. Gao, Computers Math. Applic. **45**, 731 (2003)
23. W. Hong, M. Yoon, Z. Naturforsch. A **56**, 366 (2001); B. Tian, W. Li, Y.T. Gao, Acta Mechanica **160**, 235 (2003); R. Ibrahim, Chaos, Solitons & Fractals **16**, 675 (2003); R. Ibrahim, IMA J. Appl. Math. **68**, 523 (2003)
24. W.T. Wu, J. Sys. Sci. Math. Sci. **4**, 207 (1984); W.T. Wu, Kexue Tongbao **31**, 1 (1986)
25. Z.Y. Yan, H.Q. Zhang, Phys. Lett. A **252**, 291, 1999; J. Phys. A **34**, 1785 (2001)
26. X.S. Gao, Adv. Math. **30**(5), 385 (2001, in Chinese)
27. Handbook of Mathematics Working Group, *Handbook of Mathematics*, 4th edn. (China Higher Education Press, Beijing, 1990)